Determination of terrace size and edge roughness in vicinal Si{100} surfaces by surface-sensitive diffraction

D. Saloner, J. A. Martin, M. C. Tringides, D. E. Savage, C. E. Aumann, and M. G. Lagally
Department of Metallurgical Engineering and Materials Science Center, University of Wisconsin-Madison, Madison, Wisconsin 53706

(Received 17 October 1986; accepted for publication 22 December 1986)

The capabilities of high-resolution surface-sensitive electron diffraction to determine quantitatively the terrace size, terrace size distribution, and terrace-edge roughness are explored and illustrated with measurements on a vicinal near-{100} Si surface. It is shown that terrace edge roughness can be determined with the appropriate measurement. To explain measurements on the Si surface, shadowing, terrace-edge distortion, double-height steps, unequal areas of adjoining terraces, and multiple scattering are considered. The influence of the instrument response on measurement precision is discussed.

INTRODUCTION

As the technology of surface structural defect analysis advances, it is becoming evident that many, and possibly most, surface and overlayer systems are composed of discrete regions of ordered domains. A given ordered region can be distinct from its neighbor in one or more ways. Overlayers adsorbed on a substrate can produce domains that differ by rotational or translational symmetry. Submonolayer deposition of adatoms can result in ordered overlayer islands separated by regions of bare substrate. The surface can consist of terraces at different levels separated by steps. Such systems provide experimental testing grounds for theoretical models of lower-dimensional physical behavior, such as critical phenomena, growth kinetics, and roughening transitions.

Stepped surfaces, in particular, are interesting, not only for the diversity of fundamental processes that can be studied there,[1,2] but also for their technological importance. Steps are believed to be critical in determining thin-film growth on and chemical reactivity at surfaces.[3,4] Steps occur both on singular but rough surfaces, on which the direction of the step (i.e., whether it is an "up" or a "down" step) is random, and on vicinal surfaces, on which the steps form a "staircase." The structure of thin films growing on flat surfaces can also frequently be analyzed in terms of steps between the overlayer domains and the substrate. Any quantitative investigation of the physical processes taking place in such systems rests on a determination of the size distribution of ordered domains or terraces. In this paper we discuss the determination of the distribution of terrace widths in a vicinal surface by surface-sensitive diffraction and examine the sensitivity of such a determination of terrace width distributions to the resolving power of the diffractometer. We furthermore explore the possibility of measuring edge roughness in terraces. We illustrate with results from a vicinal Si surface that has a near-{100} orientation.

Investigations of stepped surfaces to date have been restricted to one-dimensional analyses with the implicit assumption that the step edges are straight.[5] Angular distributions of intensity measured in diffraction experiments are interpreted in this limit to refer to a distribution of terrace sizes. This need not be the case, of course. Edge roughness will also affect the diffracted-intensity distribution. Thus, a given angular profile may refer to a distribution of terrace widths with straight edges or to terraces with rough edges but with the same spacing between mean edge positions. We show that a complementary measurement along an azimuth parallel to the step edge can differentiate between these two possibilities. We also show that several other phenomena associated with the existence of terraces will produce unique diffraction features. Among these are "shadowing" of portions of the terrace by the step edges, edge atom positional distortion and associated strain, and preferential growth of a given terrace type at surfaces terminating in terraces with different crystallographic symmetry.

INFLUENCE OF INSTRUMENT RESOLUTION ON TERRACE WIDTH DETERMINATION

The angular distribution of intensity diffracted from an ensemble of finite-size domains is governed by the phase relationship between domains and the structure factor of each domain. For kinematic scattering from a simple stepped surface, one can consider each terrace to have the same terrace structure factor. Then the difference d in height of the terraces determines the phase relationship between waves scattered off each terrace. When the scattering phase between terraces differs by an integral multiple of $2\pi/d$, i.e., at conditions where the normal component of the momentum transfer vector $S_\perp$ has values of $2n\pi/d$, the order appears to extend over the entire surface. At these conditions the diffracted-beam angular profiles are as narrow as the instrument can attain in $S_\parallel$, the parallel component of the momentum transfer vector. Conversely, angular profiles of diffracted beams are broadest and hence most sensitive to the terrace size at conditions $S_\perp = (2n+1)\pi/d$, at which maximal destructive interference occurs between waves scattered off terraces at different heights.

The finite energy and angular resolution of a diffractometer causes broadening of diffracted beams in $S_\parallel$ and $S_\perp$

 0021-8979/87/082884-10$02.40

(Ref. 6). For the (00) beam, the only factor causing broadening in $S_\parallel$ is the beam size at the detector. The beam size at the detector can be decreased by improving the electron optics to produce a smaller electron beam and by decreasing the detector size. The effective resolution is not given, however, by the absolute angular width of a diffracted beam, but rather by the ratio of this width to the size of the Brillouin zone (i.e., the separation of diffracted beams) and by the measurement accuracy.[6] More grazing angles provide higher resolving power.[7] Measurements reported in this paper are performed with an instrument that has a resolving power in the range of 1 μm in the plane in which the detector moves.

Consider a vicinal surface composed of regular terraces all of length M_0a with straight edges and separated by steps of height d (a "staircase"). The reciprocal lattice for such a surface, shown in Fig. 1, is well known[8] and is readily obtained in the kinematic limit as the product of the reciprocal lattice of an individual terrace with that of a superlattice of sites separated by the spacing of the individual terraces. As noted above, when the scattering phase between adjoining terraces is $2n\pi/d$ the angular profiles show no broadening and are delta functions located at the Bragg conditions in $S_\parallel$. When the phase difference is $(2n+1)\pi/d$ there is maximum interference and diffraction satellites appear at values of $S_\parallel = \pm(2m+1)\pi/M_0a$. The pattern is dominated by the satellite pairs positioned symmetrically on either side of $S_\parallel = 0$ and split by an amount $\Delta = 2\pi/M_0a$. For perfect staircase surfaces the terrace length is thus simply given by the inverse of the separation of the split satellite peaks. Note in particular that second-order satellites, at $S_\parallel = 2m\pi/M_0a$, are structure factor forbidden.

The calculation of the intensity distribution for diffraction from vicinal surfaces with monatomic steps but in which there exists a distribution of terrace widths can be performed by postulating a distribution function and evaluating the relevant autocorrelation function. For terraces where all step edges are perfectly straight in the direction perpendicular to the steps, the only contribution to deviations from the mean terrace size is from fluctuations in M_0a: the width of an entire terrace. For random fluctuations about the mean, it is reasonable to assume that the terrace widths are distributed like a Gaussian:

$$\rho(M) = (1/\sqrt{2\pi}\,\sigma)\exp[-(M-M_0)^2/2\sigma^2]\,, \qquad (1)$$

where M_0a is the average terrace width. We take the ratio of the variance of the Gaussian σ to the mean value of the Gaussian M_0 as a measure for the relative fluctuation in terrace widths. A small value of σ corresponds to a narrow-width distribution about the mean M_0. The diffraction pattern from this vicinal surface resembles that from the surface with equal-width terraces, except that the satellite beams are broadened. The quantity in the diffracted-beam profile that corresponds to σ/M_0 is w/Δ, the ratio of the full width at half maximum w of the peak and the peak separation Δ. In general, for arbitrary terrace width distributions, the shape of the satellite peaks will not be symmetrical and a comparison of experiment and theoretical models requires a fit of the entire diffracted-beam profile. However, for purposes of illustrating the influence of instrumental broadening on a determination of the terrace width distribution the dependence of w/Δ on σ/M_0 provides a good indication of the dependence of the profile shape on the parameters of the terrace width distribution. We have extracted the quantities w and Δ from angular profiles calculated for Gaussian size distributions while varying the parameters σ and M_0 of the width distribution. We incorporate instrumental broadening by assuming the instrument response function is Gaussian with a FWHM of δ and convoluting this Gaussian function with the calculated split profile. The apparent width w'/Δ of the satellite peak relative to the peak splitting is then approximately $w'/\Delta = [(\delta/\Delta)^2 + (w/\Delta)^2]^{1/2}$. This quantity is plotted in Fig. 2 as a function of σ/M_0 for several values of instrumental broadening δ. For a perfect instrument $\delta = 0$ and $w'/\Delta = w/\Delta$. The broadening of satellites relative to their separation is approximately linear with σ/M_0 for small values of the terrace width broadening σ. In the limit that σ/M_0 tends to zero we regain the case of the perfectly regular steps and the satellite peaks are delta functions. For imperfect instruments the functional dependence is more complicated. We comment on two aspects of these curves. First, for a given instrumental broadening, it is more difficult to resolve small variations in terrace width about the mean width than it is to resolve large ones. A narrower size distribution produces a narrow diffraction peak, which will be broadened by a low-resolution instrument. Second, and less obviously, a given absolute value of fluctuation in a terrace width (e.g., ± 5 atoms) is less easily resolved with a given instrument if M_0 is large than if M_0 is small. If M_0 is large the splitting of the peaks is smaller, and a poor resolution can easily wash out the splitting. Thus, advantages of a high-resolution diffractometer are apparent. Not only is high resolution impor-

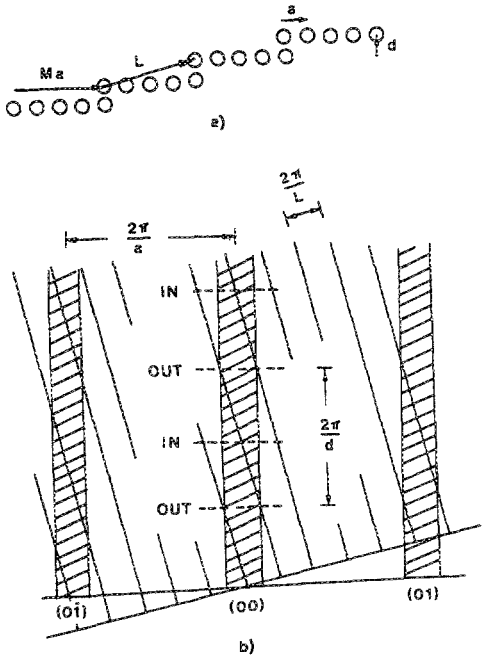

FIG. 1. Real and reciprocal-space diagrams of a vicinal surface. (a) Cross-sectional view of a regular staircase of monatomic-height steps. (b) Reciprocal lattice appropriate for the surface shown in (a). Some of the in-phase and out-of-phase scattering conditions are indicated for the (00) reciprocal-lattice rod.

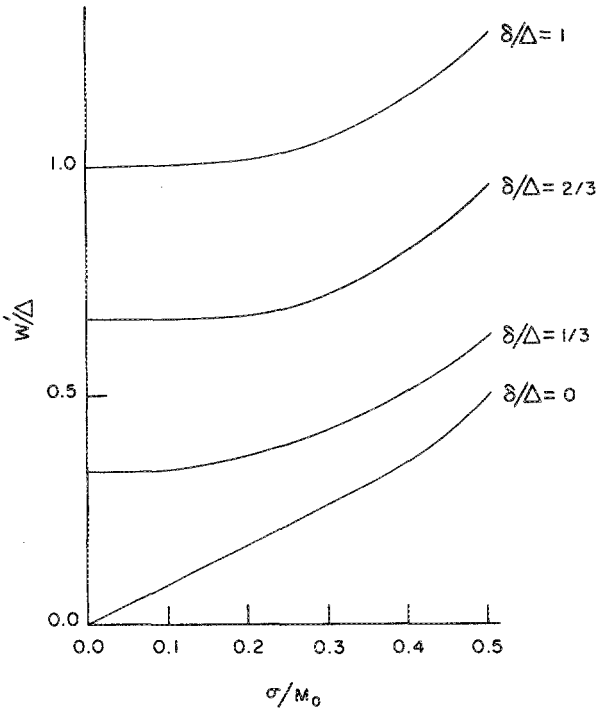

FIG. 2. Dependence of the apparent width of satellite peaks in diffraction from a vicinal surface on the terrace size uncertainty. The apparent width is plotted as a fraction of the satellite peak splitting and includes the effect of limited instrumental resolution. The terrace size uncertainty is given as a ratio of the variance to the mean of a Gaussian distribution. The several curves are for different instrumental broadening contributions δ. The figure indicates that a bad instrument prevents the observation of small variances in mean terrace sizes, and that large terrace sizes are difficult to observe with a poor instrument. The curves for w/Δ are calculated for an out-of-phase diffraction condition, $S_\perp = (2n+1)\pi/d$, at which the first-order satellite peaks appear at positions $S_\parallel = \pi M_0/a$.

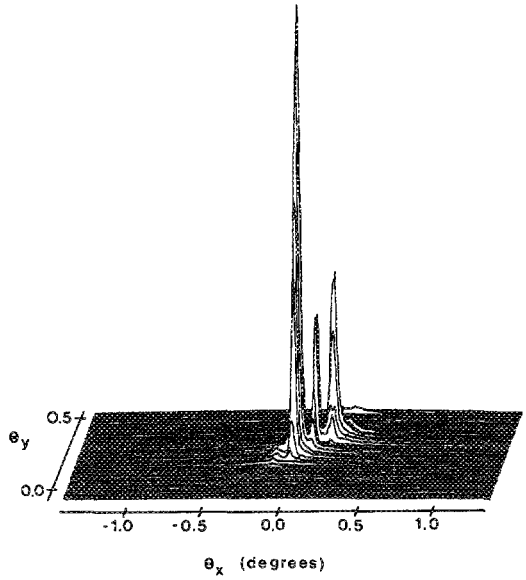

FIG. 3. Two-dimensional contour plot of the (00) beam diffracted from a nominal Si(1,1,400) surface. The measurement was made with a 50-μm-diam detector scanned in two directions over the diffracted beam. The plane made by the incident beam and the motion of the detector lies along x. Because the diffraction angles are near grazing, this is the high-resolution direction. Relative to reciprocal-lattice distances, $S_\parallel$, the scale in x is expanded with respect to y by about a factor of 7. Both x and y directions are ⟨110⟩. The direction of splitting is very nearly along y, with the scale expansion in x causing the splitting to appear to be tilted away from the y direction.

tant in resolving the splitting of the satellite peaks, thus enabling the detection of staircases with large terraces, but it increases the sensitivity of a measurement of a width distribution to fluctuations around the mean width.

The above discussion has focused on a semiquantitative analysis of the trends to be expected in the determination of terrace sizes as the relevant parameters are changed. As previously mentioned, a determination of the precise form of the size distribution requires fitting the entire measured-profile shape with a profile calculated for a specific model of the size distribution. After a brief discussion of experimental results we present such calculations of angular profiles for diffraction from surfaces with a distribution of terrace sizes.

EXPERIMENT

Measurements have been made with a high-resolving-power electron diffractometer[9] on a vicinal Si(1,1,400) surface, an orientation that is very near (001) (approx 0.2° off) and has ⟨110⟩ as a zone axis.[10] The surface was cleaned by sputter etching and subsequently annealing at temperatures of ~1100 °C for 10 min, followed by slow cooling. The electron diffractometer uses a field emission source having a beam size at the detector of ~15 μm and is capable of operating at any energy from ~150 to ~10 keV and at all angles from grazing to nearly normal. To optimize the resolving power (as described in the last section) the diffractometer is typically operated at near-grazing angles and low energy. Magnetic deflection coils are used to scan a diffracted beam across the detector, which has a 50-μm aperture. Thus, two-dimensional contour plots of the intensity in a diffracted beam can be obtained with high resolving power. Figure 3 shows an example for the (00) beam. The splitting observed in the figure is a consequence of the regular staircase of the (1,1,400) surface. With an electron diffractometer of ordinary resolution, the splitting evident in this figure would not be resolvable. If such measurements are made at different values of energy or angle of incidence, the intensities of the split peaks oscillate as is expected from a stepped surface, with a period that reflects single-atomic-height steps. Several such curves, measured in the direction normal to the step edges in the (1,1,400) surface and integrated in the orthogonal direction (as a slit detector would measure) are shown in Fig. 4. Figure 5 shows two of these profiles, at values of energy and angle that correspond to an out-of-phase and an in-phase condition for diffraction from terraces separated by single-atomic-height steps. The out-of-phase profile shows several interesting features. First, there are the two major satellites, whose separation gives the surface orientation. Additionally, however, there is a central peak and second-order satellites. We address the origin of these features in the next section.

In addition to the profiling detector, the diffractometer contains an overview detector that consists of a 5-in.-diam channel electron multiplier array and a fluorescent screen. This detector was used here only to view the diffraction pattern. Both (2×1) and (1×2) domains of reconstructed

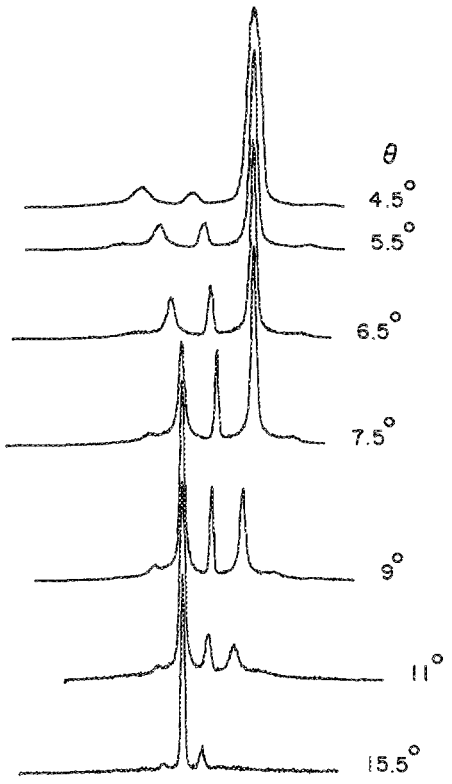

FIG. 4. Angular profiles of the (00) reflection from a vicinal (1,1,400) Si surface for different diffraction parameters. The direction of the detector motion is normal to the nominal step edges. The intensity in the direction along the step edges is integrated, i.e., these profiles reflect the measurements made with a slit detector. $E = 230$ eV. The abscissa is in arbitrary units of degrees. The angular separation of the three satellites is less than 0.5°. Peaks are arbitrarily aligned to conserve space.

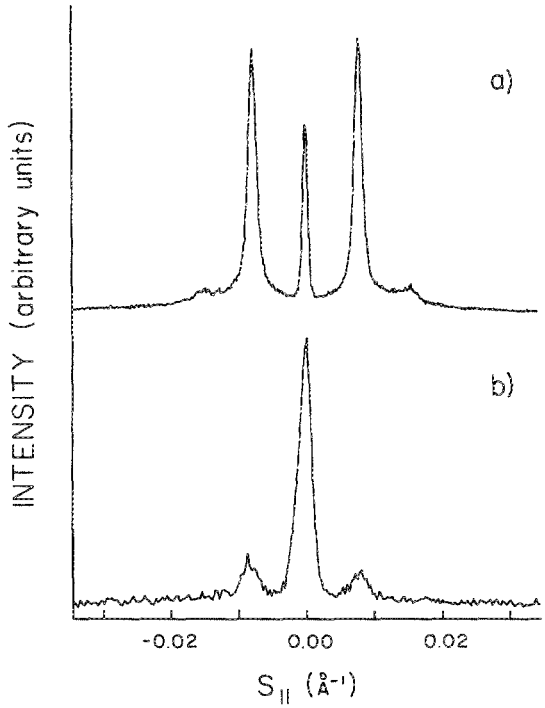

FIG. 5. Angular profiles of the (00) reflection from a vicinal (1,1,400) Si surface at (a) out-of-phase and (b) in-phase diffraction conditions for a surface with monatomic-height steps. In (a) the intensity is distributed symmetrically in the side peaks. The splitting of the strong satellite peaks indicates that the average terrace width is $\langle Ma \rangle = 2\pi/\Delta S_{\|} = 380$ Å and, for a single-layer step height ($d = 1.36$ Å), that the misorientation angle is approximately 0.2°. The in-phase profile also shows small satellites at the same splitting that suggest that multiple scattering plays a role in the scattering from terraces.

(001) surface were observed. No effort was made (unfortunately) to determine the relative intensities of the beams corresponding to the two domains.

The measurement shown in Fig. 5 is taken with the detector motion normal to the nominal step edges and with integration over the orthogonal direction. As we shall see, a measurement along the nominal step edge with integration over the direction normal to the nominal step edge (i.e., a measurement perpendicular to that shown in Fig. 5) is of considerable interest in determining step-edge roughness. Figure 6 shows such a measurement. The profile is plotted in the direction normal to the splitting direction. The data are taken from Fig. 4. Each point represents a summation of intensity in the split direction at the appropriate value normal to the split direction. This measurement shows a relatively narrow profile on top of a diffuse background. In a later section we will discuss the determination of edge roughness and make a comparison with this figure.

ANALYSIS OF PROFILES MEASURED NORMAL TO THE STEP EDGE

The profiles measured in an azimuth perpendicular to the step edge that were presented in the preceding section (Figs. 4 and 5) have several distinct features. They display split peaks, each centered a distance $\Delta/2$ in $S_{\|}$ away from the value of $S_{\|}$ at the Bragg condition. The peaks show broadening, over and above that of the instrument, reflecting the distribution of terrace widths. In addition to the first-order satellite peaks that are expected from the simple diffraction analysis described earlier, peaks appear at the value of $S_{\|}$ satisfying the Bragg condition and at the second-order satel-

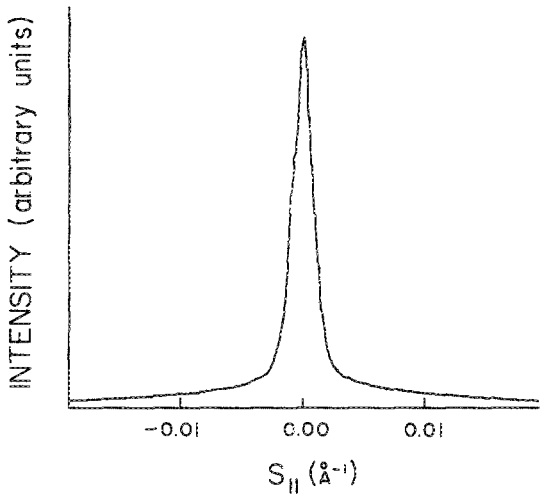

FIG. 6. Angular profile of the (00) beam from a vicinal (1,1,400) Si surface with the measurement direction along the nominal step edge and integration over the intensity in the orthogonal direction. The profile thus reflects the measurement that would be obtained with a slit detector. The curve is obtained from the data shown in Fig. 3.

lite positions. Several factors could cause these features, and these are discussed below. We ignore these complications for the moment, and first determine the average terrace width from the splitting and the nominal terrace size distribution from the broadening. The mean terrace size is simply obtained from $\langle Ma \rangle = 2\pi/\Delta = 380$ Å. The distribution of terrace widths about this mean value can be obtained by fitting the angular profile of the first-order satellites with a model of the terrace width distribution. Using the model described in the second section, that the terrace widths are Gaussian distributed with a mean value $M_0 a$ and a standard deviation σ, and assuming the terrace edges are smooth, we get $\sigma = 110$ Å. In other words, the average terrace size is $\sim 380 \pm 110$ Å.

We now address the origin of the second-order satellites and the central peak in the profile shown in Fig. 5(a). There are five different effects that we know of that may cause one or the other or both of these features. These are (1) double-atomic-height steps, (2) shadowing, (3) edge atom positional distortion, (4) (2×1) and (1×2) terraces of different total area, and (5) equal-area terraces having a different terrace structure factor. We address these in turn. We note at this stage that a limited instrumental response leading to integration of intensity over a range in $S_\perp$ (Ref. 6) cannot cause these features. The instrument can only cause broadening of features in these profiles. We can also, without further discussion, put an upper limit of $\sim 20\%$ on the percentage of steps that can be double-atomic-layer-height steps, because the angular profiles show oscillatory behavior in $S_\perp$ that corresponds to single-height steps. We also observe both (2×1) and (1×2) patterns.

In configurations where the incident or exit beams are normal to the step edge and make a small angle with the terrace plane, there will be a portion of the terrace that is "shadowed," and thus blocked from contributing to the diffracted beam. When the beam is directed down the staircase, only part of each terrace is illuminated. When the beam is directed up the staircase, a portion of the scattered beam must penetrate the step edge to reach the detector. Shadowing reduces the effective width of the scattering terraces. (It effectively leaves "dead space" that does not contribute to the scattering.) This moves the zero of the structure factor from the position of the second-order satellite and the corresponding peak is no longer suppressed. The intensity in the second-order satellite is governed by the extent of shadowing. This can be an important effect for measurements made at small angles, as in RHEED and grazing-angle x-ray diffraction. It also holds some promise as a means for studying edge-atom thermal vibrations by examining the shadowing effect as a function of substrate temperature via the intensity in the second-order satellite. Shadowing does not produce a peak at $S_\parallel = 0$.

It is similarly possible to observe a second-order satellite peak if edge-atom positional distortion exists. The possibility of measuring edge-atom displacement from regular lattice sites from shifts in the oscillation period of angular profiles with $S_\perp$ has been discussed.[11,12] The displacement of some fraction of the atoms in a terrace from their regular lattice sites effectively modifies the length over which order exists in each terrace. Edge-atom displacement will produce a strain field because of the resultant asymmetric forces exerted on the neighboring atoms, which can extend for some distance through the terrace. Depending on the magnitude of the displacements of atoms near the terrace edge, the structure factor of each terrace will be modified such that the structure factor no longer suppresses the second-order satellite peak, but no peak is produced at $S_\parallel = 0$.

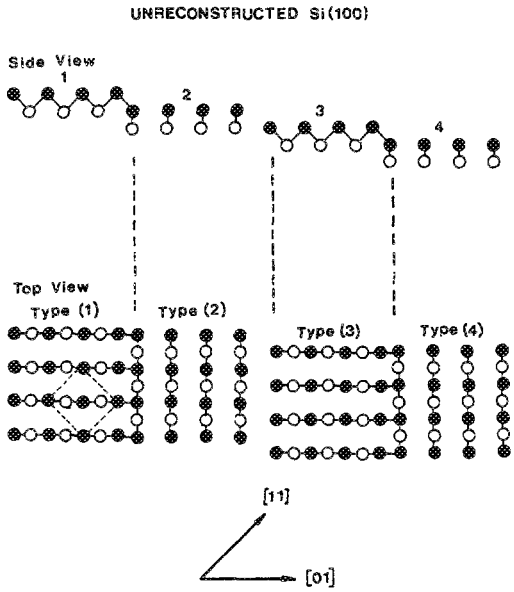

FIG. 7. Schematic illustration of the four possible terminations of unreconstructed Si(100). Filled circles represent surface atoms; open circles are subsurface atoms. The dashed box indicates a face of the fcc unit cell. Directions in the surface are indicated, using 2D (surface) notation. Note that the [01] direction in the surface notation corresponds to the [011] direction in 3D notation. The solid lines between atoms represent covalent bonds.

The fourth mechanism we discuss is one that can produce peaks both at the Bragg condition and at the second-order satellite position. For systems, such as Si(100), that have an ABCD... stacking and a consequent ABAB... order on adjacent terrace (see Fig. 7), it is possible that growth of one of the domain types A or B is preferred, with the consequence that the mean terrace width of domain type A is different from that of domain type B. This will result in a peak at the Bragg condition $[S_\parallel = 0]$ proportional to $|\langle M_A \rangle f_A - \langle M_B \rangle f_B|^2$. Because the structure factors of adjacent terraces are now not equal, second-order satellites are also possible.

Finally, we consider the fifth possibility, which can be understood with the aid of Fig. 7. When there are steps on the Si(001) surface, no matter what their orientation, the exposed terraces are not identical when viewed along a $\langle 110 \rangle$ azimuth. The rotational symmetry, shown in Fig. 7, results in an effective ABAB... terrace-type sequence. In a separate paper[13] we show that multiple scattering causes the scattering factors of unit cells in terrace A to be in general different from those in terrace B except in special directions and for special reflections. Diffraction experiments on a sputter-etched and annealed singular Si(001) surface show double-height steps when measured along a $\langle 110 \rangle$ direction and single-height steps when measured along a $\langle 100 \rangle$ direc-

tion, in which the dynamic structure factors are shown to be equal.[13] The only justifiable explanation for the observed phenomenon is multiple scattering.[13] A difference in scattering factors of unit cells in terrace A and those in terrace B is sufficient for the appearance of a peak at the Bragg condition. However, in the simplest analysis that assumes uniform terrace sizes and includes only double scattering, the peak at the second-order satellite is still suppressed.

The presence of second-order satellites and a central peak at the Bragg condition in diffraction from a vicinal surface can thus be interpreted in the framework of several different models. By fitting the measured profile (Fig. 5) with each of the models, one can estimate whether they are reasonable in this situation.

For shadowing to account for the magnitude of the second-order satellites, 20% of the scatterers on a terrace would need to be shadowed. At the conditions of the experiment, only about 3% of the atoms are geometrically shadowed. Thus, it seems unlikely that shadowing is responsible for all of the intensity of the second-order satellites. In any case, the peak at $S_{\parallel} = 0$ is not reproduced.

We have modeled edge atom positional distortion by assuming an edge-atom displacement of αd perpendicular to the surface and βa parallel to the surface, where α and β are constants. We further assume that the resultant motion causes a displacement of N of the neighboring atoms that is linearly proportional to their distance from the edge atom, i.e., for the nth atom from the edge there will be a movement of $\alpha\ (N + 1 - n)d/N$ perpendicular to the surface and $\beta\ (N + 1 - n)a/N$ parallel to the surface. To reproduce the experimental profile of Fig. 5(a), very large strains are needed, with typical values of N, α, and β being $N/M_0 = 20\%$, $\alpha = 15\%$, $\beta = 15\%$. This seems unreasonable. Edge atom displacement will clearly cause a more noticeable effect for smaller mean terrace widths. The central peak is not reproduced.

The central peak can be matched if the structure factors are assumed unequal because of multiple scattering[13]; however, no second-order satellites appear in our simple model. A calculation is shown in Fig. 8. A ratio of terrace structure factors $f_A/f_B > 2$ must be assumed to fit the relative intensities of the central peak and the first-order satellites in Fig. 5(a).

Second-order satellites and a small central peak occur if the structure factor differences are due to differences in the number of atoms on terrace types A and B. However, the relative peak magnitudes observed in the experiment cannot be fitted unless multiple scattering is also included. The best fit is obtained if unequal terrace sizes with a terrace area (width) ratio of $M_A/M_B = 11/8$ and a structure factor ratio $f_A/f_B = 2$ is assumed. The resultant fit is shown in Fig. 9.

To aid in determining the correct model for a given surface it is necessary to extend the analysis to different diffraction conditions. Several such conditions are shown in Fig. 4. Particularly the profile shape at the in-phase conditions [Fig. 5(b)], for which small satellites are still present, allows us to eliminate the model that consists of the combination of unequal A and B terrace areas and the existence of some double-height steps. The existence of satellites at the in-phase conditions further suggests that multiple scattering plays a role. Other factors can also be investigated by varying $S_{\perp}$. In particular, the influence of shadowing can be varied by varying the diffraction geometry. For a given configuration of the incident beam, sample, and detector the angular profile obtained for a given beam at higher-order out-of-phase conditions should be unchanged. This will clearly not be the case for step-edge atom displacement, for which the phase relationship between atoms shifted from the regular lattice sites and those in regular lattice sites will vary with the value of $S_{\perp}$. If the only factor present is a difference in the mean widths of the two terrace types then the angular profiles will

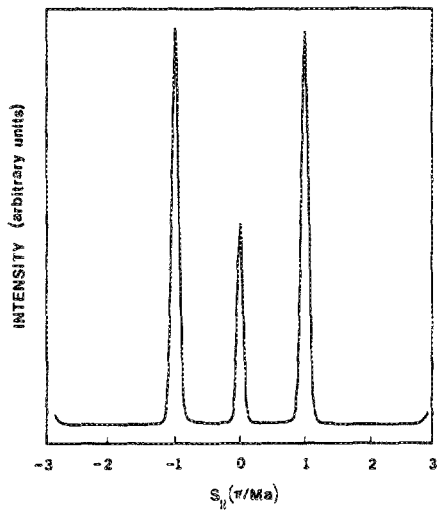

FIG. 8. Calculation of the angular profile corresponding to the measurement shown in Fig. 5(a) if multiple scattering is assumed to change the structure factors of adjacent terraces. In this calculation, the dynamic structure factors of adjacent terraces have a ratio $f_A/f_B = 2$. All other conditions are the same as in the experiment.

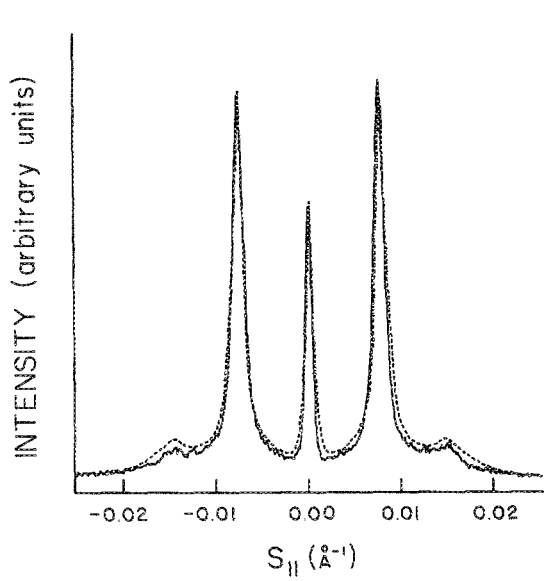

FIG. 9. Calculated fit to the curve in Fig. 5 using unequal-size terraces for type A and type B terraces and unequal terrace structure factors. The ratio of structure factors is $f_A/f_B = 2$. The ratio of terrace areas is 11:8. It is not possible to specify which type of terrace is the one with the larger area from the fit to angular profiles.

be unchanged both with the order of the out-of-phase condition and with the geometry of the incident beam, sample, and detector. This latter condition is not fulfilled at least on singular Si(001) surfaces,[13] for which there is a definite azimuthal dependence, suggesting that a multiple-scattering effect is involved.

ANGULAR PROFILES AND STEP EDGE ROUGHNESS

In this section we will address the use of angular profiles in diffraction from regularly stepped surfaces to determine the terrace width distribution and terrace-edge roughness. We do this by considering diffraction for different orientations relative to the step direction. We first consider diffraction with the beam incident perpendicular to the (nominal) step edge, as in the experiments analyzed in the last section. We assume the detector measures the angular distribution of intensity in the plane perpendicular to the step edge and integrates the intensity in the diffracted beam parallel to the step edge. The measured angular profile is then sensitive to the succession of strings of atoms sampled in a one-dimensional cut across the surface perpendicular to the step edge and averaged over all such cuts.[14] We restrict ourselves to cases where the mean terrace edges are widely enough separated, relative to any fluctuations in the terrace edges, that the fluctuations at one terrace edge can be considered to be independent of those in the neighboring terrace edges. We define the length of the crystal in the direction parallel to the mean step edges to be L_c. Within a terrace of area A, the mean width perpendicular to the step edge is $\langle Ma \rangle = A/L_c$. For a rough-edged terrace, different strings of atoms have different lengths Za perpendicular to the mean step edge. The string length distribution $P(Z)$ is then a folding of the probability $\rho(M)$, of having a terrace of a certain width Ma, with the probability $p(M,Z)$, of having a string length, Z in this terrace:

$$P(Z) = \int \rho(M) p(M,Z) dM . \tag{2}$$

We now consider two specific cases. First, for smooth terrace edges, but a Gaussian distribution of terrace widths, Eq. (1) applies:

$$\rho(M) = \frac{1}{\sqrt{2\pi}\sigma} \exp\left(- \frac{(M - M_0)^2}{2\sigma^2} \right)$$

and

$$p(M,Z) = \delta(M - Z) . \tag{3}$$

The integral of Eq. (2) yields

$$P(Z) = \frac{1}{\sqrt{2\pi}\sigma} \exp\left[- (Z - M_0)^2 / 2\sigma^2 \right] . \tag{4}$$

Second, for terraces with a constant width ($M = M_0$) but with rough edges whose excursions are Gaussian distributed, we have

$$\rho(M) = \delta(M - M_0) \tag{5}$$

and

$$P(M,Z) = \frac{1}{\sqrt{2\pi}\sigma} \exp\left[- (Z - M)^2 / 2\sigma^2 \right] . \tag{6}$$

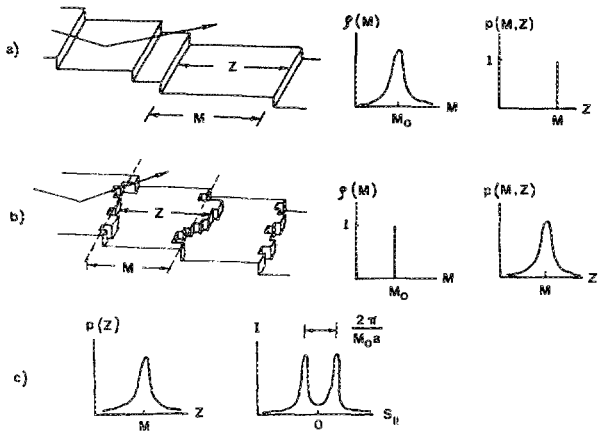

FIG. 10. Schematic illustration that diffraction cannot uniquely detect step-edge roughness in vicinal surfaces when the scattering plane is perpendicular to the step-edge direction. Width probability functions for (a) an array of steps that have random terrace sizes but smooth step edges are complementary to the width probability functions for (b) an array of steps with constant mean terrace width but rough step edges. The two cases result in (c) identical string length and intensity distributions.

The integral of Eq. (2) again yields

$$P(Z) = \frac{1}{\sqrt{2\pi}\sigma} \exp\left[- (Z - M_0)^2 / 2\sigma^2 \right] . \tag{7}$$

The equality of Eqs. (4) and (7) demonstrates that the diffracted-beam profiles for these two cases must be identical. This is shown in Fig. 10 together with the real-space configuration and respective terrace size distributions. Thus, for measurement with a slit detector perpendicular to the mean step edge, it is not possible to differentiate between staircases that have terraces of constant width but with rough edges

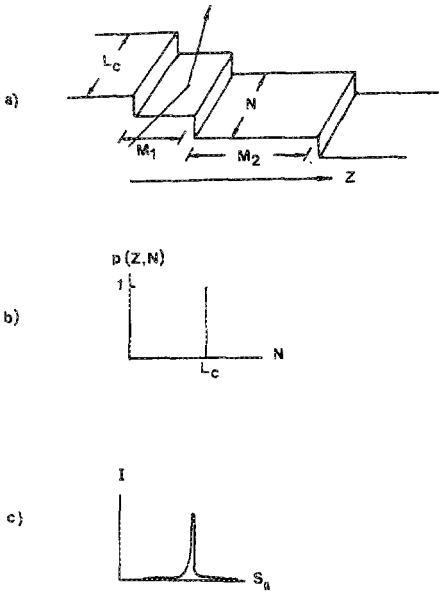

FIG. 11. Schematic illustration of diffraction from a vicinal surface with smooth terrace edges and variable terrace width with the scattering plane aligned with the step-edge direction. The diffraction is sensitive to string lengths at various positions Z. Because all strings have length L_c, the string length distribution (b) is a delta function and the intensity (c) will be sharply peaked with a width inversely related to L_c. The drawing in (a) is not to scale: L_c is assumed much larger than M.

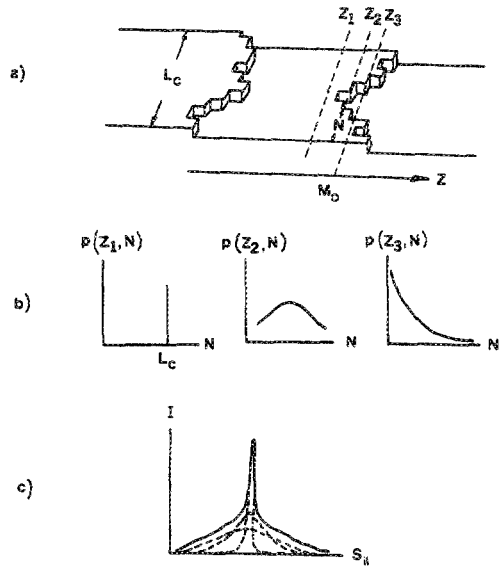

FIG. 12. Illustration that measurement of diffraction from a stepped surface with the scattering plane along the direction of the nominal step edges and the intensity integrated over the perpendicular direction reflects the edge roughness. (a) The diffraction is sensitive to the various string lengths N at positions $\pm Z$ about the mean terrace width M_0. String lengths vary from one atom to L_c. (b) Examples of three distributions of string lengths at positions Z_1, Z_2, and Z_3. (c) Intensity profile produced by the sum of the cuts at different positions has broad components from positions where the string lengths are short (e.g., Z_2) and narrow components at positions where the string lengths are long (e.g., Z_1). The drawing in (a) and the abscissas in (b) are not to scale; L_c is assumed to be much larger than the dimension of a double kink. Only the probability functions for atoms in the (↑) terrace are shown. Note that in the calculation shown in Fig. 9, probability distributions such as those shown in (b) for Z_2 were not included. The profile was calculated with distributions for Z_1 and various values for Z_3. This creates a negligible error.

and staircases that have terraces with smooth edges but variable width. However, angular profiles measured parallel to the step edges (with integration over the diffracted intensity perpendicular to the profiling azimuth) will be sensitive to the differences in these two terrace structures. When the step edges are smooth, all string lengths are equal to L_c, the length of the crystal parallel to the step edges. The scattering geometry is shown in Fig. 11(a), with the corresponding length probability function and intensity distribution shown schematically in Figs. 11(b) and 11(c), respectively. For a surface with constant mean terrace size ($M = M_0$), but with terrace edges that are rough, a cut at position Z in a direction parallel to the mean edge (located at $M_0 a$) will, in general, contain atoms from two adjacent terraces (and, hence, at different heights), and thus short strings of atoms that are in a given terrace. The diffraction profile at the out-of-phase condition is a sum of the contributions from each cut, which will contribute a distribution of string lengths $p(Z,N)$ over which consecutive atoms are in the same terrace. This can be seen in Fig. 12(a). Note that strings in both adjacent terraces contribute. Cuts that are far from the mean edge $M_0 a$ will contribute to a narrow peak and a very diffuse background in the angular profile, reflecting the large average length of a string before encountering an atomic step and then a very short string. The narrowest contributions come from strings with length L_c. Contributions from cuts nearer to the mean edge contribute a broader profile, because of the correspondingly small average string length before a step is encountered. The total diffracted intensity will be a sharp peak with diffuse wings. The wings will be wider the rougher the step edge. The ratio of the integrated intensity in the diffuse wings and that in the sharp peak reflects the magnitude of the excursion of the step edge from the mean position. A calculation of the angular profiles of the diffracted beams requires that the distribution of lengths $p(Z,N)$ sampled in each of the cuts at different Z be specified. Figure 12(b) schematically illustrates $p(Z,N)$ for the several values of Z indicated in Fig. 12(a). The corresponding individual string contributions to the intensity are shown as the dashed lines in Fig. 12(c) with the total intensity from all contributions indicated by the solid line.

The preceding discussion establishes qualitatively that step-edge roughness can be distinguished from terrace size variation in vicinal surfaces by analysis of angular profiles collected in complementary directions. Edge roughness will produce "wings" on angular profiles collected with the scattering direction parallel to the mean step edges that should be detectable with high-resolving-power instruments.

A quantitative calculation of the angular profiles of the diffracted beams requires the specification of two string-length distributions in adjacent terraces. There are situations where the string lengths in a cut at Z are related to the lengths in a cut at $Z + 1$ and this will affect the shape of the profile.[14] In order not to obscure the discussion of edge roughness we assume statistical independence of the string lengths. We further assume that both string-length distributions are geometric, i.e.,

$$P_{\uparrow\downarrow}(Z,N) = \gamma_{\uparrow\downarrow}(Z)\,[1-\gamma_{\uparrow\downarrow}(Z)]^{N-1}, \tag{8}$$

where ↑ and ↓ refer to two adjacent terraces separated by one atomic-step height and $\gamma(Z)$ is the probability of finding a string of a certain length at position Z and is thus a measure of edge roughness. Rougher edges give larger values of γ. If the probability of an excursion from the mean terrace width is Gaussian distributed, the effective coverage of a cut at a distance Z' from the mean edge $-M_0/2 < Z' < M_0/2$ by atoms from one terrace (↑) is given by

$$\theta_{\uparrow}(M_0,Z') = 1 - \int_{-M_0/2}^{Z'} [p(M_0,x+M_0)]^{1/2}\,dx \tag{9}$$

and the coverage by atoms of the other terrace (↓) is

$$\theta_{\downarrow}(M_0,Z') = 1 - \theta_{\uparrow}(M_0,Z')\,. \tag{10}$$

The value of γ in Eq. (8) for the two adjacent terraces can then be evaluated in terms of Eqs. (9) and (10) by recognizing that

$$\gamma_{\uparrow} = \gamma_{\downarrow}(1-\theta_{\uparrow})/\theta_{\uparrow}\,. \tag{11}$$

Using the model of Eqs. (8), (9), and (11), we can fit the angular profile shown in Fig. 6. To fit the profile requires using a Gaussian-distributed step-edge roughness that ranged in values of Z from approximately $0.7\,M_0 < Z < 1.3\,M_0$. In other words, the uncertainty in the mean terrace width, $\langle Ma \rangle = 380 \pm 110$ Å calculated for Si(1,1,400) can be essentially all attributed to terrace-edge roughness.

In summary, the determination of terrace width distri-

butions and an evaluation of the terrace edge roughness can in principle be achieved by an analysis of angular profiles measured in complementary directions from a stepped surface.

DISCUSSION AND CONCLUSIONS

Surface-sensitive diffraction with high-resolution diffractometers is a powerful technique to investigate the quality and roughness of vicinal surfaces. We have demonstrated that high resolution allows one to determine more quantitatively the nature of the terrace size distribution. We have shown that diffraction profiles from stepped surfaces contain features that can be analyzed in terms of such surface effects as edge atom distortion or the preferential existence of one terrace type over another in surfaces where more than one type exists, and in terms of diffraction effects such as beam shadowing or multiple scattering. We have briefly indicated how one might distinguish between these influences.

We have furthermore shown that complementary measurements made parallel and perpendicular to the step edge can in principle distinguish between terrace-edge roughness and terraces that have smooth edges but a distribution in widths. Such a measurement suggests the possibility of measuring roughening transitions in terrace edges[2,5] by following the temperature dependence of the edge roughness. A low-resolution diffractometer is sensitive only to correlations over a short distance, and thus preferentially sees only the local disorder that occurs when the temperature is still far from the roughening temperature. A high-resolution measurement will probe the long-range correlations that are due to terrace edge meandering, and thus will allow a closer approach to the actual roughening temperature.

With respect to our measurements on Si(1,1,400), we are left with a somewhat incomplete picture that at the moment leaves us a choice of at least two explanations. On singular sputter-etched and annealed Si(100) surfaces,[13] we observe an azimuthal dependence of the angular profile (single-height versus double-height steps) that can be explained, we believe, only by multiple scattering. We expect the same effect here. Unfortunately, the azimuthal-dependence measurement has so far not been made on Si(1,1,400).

Multiple scattering can explain[13] a number of observations in the literature. For example, Sakamoto *et al.*[15] observe two different oscillation periods (single-height steps and double-height steps) whose existence depends on the azimuthal orientation with respect to the electron beam. This is just as we observe.

Multiple scattering could be the only factor in Si(1,1,400) if one could explain the existence of the second-order satellites. The simplest analysis of multiple scattering maintains a zero in the structure factor at the position of the second-order satellites. One can imagine that multiple scattering can remove the zero and give intensity here in the same manner that forbidden reflections appear in x-ray diffraction.

The alternative explanation, of course, is that area differences in type A terraces and type B terraces cause the observed profiles. A factor of 50% difference in the areas of the two types provides a reasonable fit to the second-order satellites but gives too low an intensity at the $S_{\parallel} = 0$ peak. The notion that one type of terrace is preferred over the other is not new. Kaplan[16] suggested this possibility as one alternative in interpreting his LEED measurements on vicinal Si surfaces cut with a ⟨110⟩ zone axis, as are ours. He observed only the (2×1) reconstruction for large misorientation angles (6–10°). He suggested that terraces that should show the (1×2) reconstruction either were absent or did not support the reconstruction. The latter appears physically reasonable, because the terraces are only several atoms wide. If the former were true he should observe oscillations corresponding to double-atomic-height steps. He did make measurements of the oscillation in beam profile splitting with energy[8] to check for step height, and found double-height steps. Unfortunately he reported measurements only on the (01) beam, which, due to the crystal structure of Si, has fewer forbidden reflections in S_1 than the (00) beam and thus always gives a modulation that appears as a double-height step. One cannot therefore distinguish which of the two possibilities for the absence of a (1×2) superlattice is the correct one on the basis of the reported measurements.

Recently, it has been again suggested[17] that terraces with the (1×2) reconstruction on vicinal Si surfaces with ⟨110⟩ zone axes are absent, on the basis of a calculation that shows that these terraces are very slightly less stable, a consequence of the bonding arrangement at the step edge. The absence of one kind of terrace leads to double-height steps. The (1×2) reconstruction is, of course, also the one that is not observed in Kaplan's work.[16] It is suggested[17] that high-temperature annealing ($\sim$1100 °C) is required to obtain the pure double-height structure.

Our results give some support for this model. Our measurements are made on a surface that is much closer to singular than those of Kaplan. We do observe both terrace types. Our annealing conditions are $>$1100 °C for 10 min, for which we should expect[17] only double-height steps on the basis of the new model. Our fit gives a ratio of terrace areas of 11:8. We cannot tell from the angular profiles which terrace type is predominant. We should be able to tell from the relative intensities of the (1×2) and (2×1) diffraction patterns. Visual observation showed no difference, but this is probably not surprising, as a factor of 2 in integrated intensity and a factor of 4 in peak intensity are probably not resolvable by eye, especially since variations in intensity with diffraction conditions are much larger than that. Accurate intensity measurements have not been made.

One could suggest that our measurements show so far the strongest support for the absence of one type of terrace, and that the fact that both exist may be due to kinetic limitations, since the terraces are very large and it takes considerable mass transfer to eliminate one in favor of the other. There is, however, so far no direct evidence that double-height steps dominate on vicinal Si(100), the strongest evidence being Kaplan's reported absence of a (1×2) pattern. However, with terraces only 5–10 atoms wide, Kaplan's suggestion that terraces this narrow cannot support reconstruction is entirely reasonable, especially in light of similar reports on W(100) (Ref. 18).

In order to address these questions more fully, experiments are in progress[19] on vicinal surfaces with other orientations, and on the temperature dependence of edge roughness.

ACKNOWLEDGMENTS

We acknowledge useful discussions with W. Moritz, M. B. Webb, and P. K. Wu. This research was supported by NSF, Solid State Chemistry Program, Grant No. DMR 83-18601, and in part by U.S.-Spain Joint Committee for Technological Cooperation.

[1]B. E. Clements and P. Kleban, Surf. Sci. **138**, 211 (1984).
[2]E. H. Conrad, R. M. Aten, D. S. Kaufman, L. R. Allen, and T. Engel, J. Chem. Phys. **84**, 1015 (1986).
[3]J. M. Van Hove, C. S. Lent, P. R. Pukite, and P. I. Cohen, J. Vac. Sci. Technol. B **1**, 741 (1983).
[4]S. Ferrer, J. M. Rojo, M. Salmeron, and G. A. Somorjai, Philos. Mag. A **45**, 261 (1982).
[5]Exceptions to this generality are the recent investigations of step-edge roughening using atomic-beam diffraction. See Ref. 3 and also J. Villain, D. Grempel, and J. Lapujoulade, J. Phys. F **15**, 809 (1985).
[6]M. G. Lagally, in *Methods of Experimental Physics: Surfaces*, edited by R. L. Park and M. G. Lagally (Academic, Orlando, FL, 1985).
[7]J. M. Van Hove, P. Pukite, P. I. Cohen, and C. S. Lent, J. Vac. Sci. Technol. A **1**, 609 (1983).
[8]M. Henzler, in *Electron Spectroscopy for Surface Analysis* (*Topics in Current Physics*, Vol. 4) edited by H. Ibach (Springer, Berlin, 1977).
[9]M. G. Lagally and J. A. Martin, Rev. Sci. Instrum. **54**, 1273 (1983).
[10]The orientation of the surface is actually azimuthally rotated slightly off (1,1,400). If it were strictly (1,1,400), the nominal terrace edges would have ⟨110⟩ directions. From the diffraction measurements we determine that the nominal terrace edges consist of approximately 10 atom ledges separated by a kink. A more precise orientation is (11,7,3750).
[11]A. J. Algra, S. B. Luitjens, E. P. Th. M. Summeijer, and A. L. Boers, Phys. Lett. **75A**, 496 (1980).
[12]M. Henzler and J. Clabes, Jpn. J. Appl. Phys. Suppl. 2, Part 2, 379 (1974).
[13]J. A. Martin, C. E. Aumann, D. E. Savage, M. C. Tringides, M. G. Lagally, W. Moritz, and F. Kretschmar, J. Vac. Sci. Technol. A (to be published).
[14]D. Saloner, P. K. Wu, and M. G. Lagally, J. Vac. Sci. Technol. A **3**, 1531 (1985).
[15]T. Sakamoto, N. J. Kawai, T. Nakagawa, K. Okta, and T. Kojima, Appl. Phys. Lett. **47**, 617 (1985).
[16]R. Kaplan, Surf. Sci. **93**, 145 (1980).
[17]D. E. Aspnes and J. Ihm, Phys. Rev. Lett. **57**, 3054 (1986).
[18]G. C. Wang and T.-M. Lu, Surf. Sci. **107**, 139 (1981); **122**, L635 (1982).
[19]A preliminary report of this work was presented at the National Symposium of the American Vacuum Society, October 1985 (unpublished).